

RESEARCH ARTICLE

SIJAZ10 and *SIJAZ11* mediate dark-induced leaf senescence and regenerationBoyan Tang^{1,2}, Tingting Tan^{1,2}, Yating Chen^{1,2}, Zongli Hu^{1,2}, Qiaoli Xie^{1,2}, Xiaohui Yu^{3*}, Guoping Chen^{1,2*}

1 Key Laboratory of Bioengineering Science and Technology, Chongqing University, Ministry of Education, Chongqing, China, **2** Bioengineering College, Campus B, Chongqing University, Chongqing, People's Republic of China, **3** Hainan Key Laboratory for Sustainable Utilization of Tropical Bioresources, College of Tropical Crops, Hainan University, Haikou, People's Republic of China

* xiaohuiyu@hainanu.edu.cn (XY); chenguping@cqu.edu.cn (GC)



OPEN ACCESS

Citation: Tang B, Tan T, Chen Y, Hu Z, Xie Q, Yu X, et al. (2022) *SIJAZ10* and *SIJAZ11* mediate dark-induced leaf senescence and regeneration. *PLoS Genet* 18(7): e1010285. <https://doi.org/10.1371/journal.pgen.1010285>

Editor: Li-Jia Qu, Peking University, CHINA

Received: March 2, 2022

Accepted: June 7, 2022

Published: July 13, 2022

Copyright: © 2022 Tang et al. This is an open access article distributed under the terms of the [Creative Commons Attribution License](https://creativecommons.org/licenses/by/4.0/), which permits unrestricted use, distribution, and reproduction in any medium, provided the original author and source are credited.

Data Availability Statement: All relevant data are within the manuscript and its [Supporting Information](#) files.

Funding: This work was supported by the National Natural Science Foundation of China (no.31872121, 31960526) and the Natural Science Foundation of Chongqing of China (csts2019jcyj-msxmX0094). The funders had no role in study design, data collection and analysis, decision to publish, or preparation of the manuscript.

Competing interests: The authors have declared that no competing interests exist.

Abstract

During evolutionary adaptation, the mechanisms for self-regulation are established between the normal growth and development of plants and environmental stress. The phytohormone jasmonate (JA) is a key tie of plant defence and development, and JASMONATE-ZIM DOMAIN (JAZ) repressor proteins are key components in JA signalling pathways. Here, we show that JAZ expression was affected by leaf senescence from the transcriptomic data. Further investigation revealed that *SIJAZ10* and *SIJAZ11* positively regulate leaf senescence and that *SIJAZ11* can also promote plant regeneration. Moreover, we reveal that the SIJAV1-SIWRKY51 (JW) complex could suppress JA biosynthesis under normal growth conditions. Immediately after injury, *SIJAZ10* and *SIJAZ11* can regulate the activity of the JW complex through the effects of electrical signals and Ca^{2+} waves, which in turn affect JA biosynthesis, causing a difference in the regeneration phenotype between *SIJAZ10-OE* and *SIJAZ11-OE* transgenic plants. In addition, SIRbcs-3B could maintain the protein stability of *SIJAZ11* to protect it from degradation. Together, *SIJAZ10* and *SIJAZ11* not only act as repressors of JA signalling to leaf senescence, but also regulate plant regeneration through coordinated electrical signals, Ca^{2+} waves, hormones and transcriptional regulation. Our study provides critical insights into the mechanisms by which *SIJAZ11* can induce regeneration.

Author summary

In plants, senescence is the final stage of development, but regeneration can help them beyond the stage. Plants regeneration is essential for propagation, and in cultivated crops to maintain excellent traits as close as possible. JA signaling can sense environmental signals and integrate various regulatory mechanisms to ensure plants regeneration occurs under optimal conditions. In this work, the JAZ-JAV1-WRKY51 complexes with reported was further optimized, the function of *SIJAZ10* and *SIJAZ11* was identified to promote inhibitory activity of SIJAV1-SIWRKY51 complex which negatively regulated JA biosynthesis by direct binding of the W-box of the *SIAOC* promoter. The results of further

investigation suggest that the differences in regulation of electrical signals, Ca²⁺ waves, hormones and transcriptional regulation are responsible for the regeneration between SIJAZ10 and SIJAZ11. In addition, we have found that SIRbcs-3B could maintain the protein stability of SIJAZ11 to protect it from degradation. In summary, despite both SIJAZ10 and SIJAZ11 can function as senescence, only SIJAZ11 has an important promoting function for regeneration.

Introduction

Leaf ageing, eventually senescence or structural damage of leaf structures, is a crucial link of later stages in plant growth and development [1]. Leaf senescence is not simply a termination phase for leaf life, but also is more of a programmed plan for nutrient relocation within the plant [2–4]. A series of complex changes in physiology, biochemical metabolism, hormone levels, and gene regulation are accompany leaf senescence [5]. Generally, leaf senescence has been divided into leaf senescence-developmental (natural) leaf senescence and stress-induced leaf senescence. Natural leaf senescence is an age-dependent process and preludes to leaf death [6], while stress-induced leaf senescence is induced by an external stimulus [7]. Stress-induced leaf senescence may induce premature senescence and even affect plant growth, which can lead to a decrease in plant yield and quality [8, 9]. Moreover, prolonged darkness is a well-known powerful external stimulus capable of accelerating leaf senescence [10].

Plant regeneration is a unique phenomenon credited to cellular totipotency. Regeneration capacity is associated with cellular senescence and ageing, which are frequently associated with wound signals [11]. Plant regeneration involves the stimulation of exogenous plant hormone signalling, the division of quiescent cells, and formation of meristems or organ primordia in vitro [12]. The molecular crossroads between stress responses and regeneration have begun to be studied in recent years. During regeneration after injury, jasmonic acid immediately accumulates and activates ERF109 (ETHYLENE RESPONSE FACTOR109). Immediately afterwards, ERF109 upregulates ASA1 (ANTHRANILATE SYNTHASE α 1) which can mediate lateral root formation. Hours later, ERF109 initiates a regulatory feedback loop to repress JA signalling pathways by directly interacting with JASMONATEZIM-DOMAIN (JAZ) proteins [13–16].

Jasmonate has been well recognized as a plant-defending hormone involved in leaf senescence, regeneration, abiotic stress response, wounding and pathogen responses [17–20]. Ros, calcium, and electric signals are the key mediators of rapid signals in response to ageing [17]. JA has been demonstrated to be a vital signal that triggers plant responses against abiotic stress and pathogen infection [21]. JA not only can interact with auxin, gibberellin and ethylene to regulate leaf senescence [22], but also serves as a potent regulatory lipid in response to stress [23]. By adjusting the relative JA contents in wounds and in undamaged distal tissues, the plant-defence systems are activated against various stresses [24]. The latest literature has revealed that wounding and JA are the first events triggering regeneration [24–27].

The biologically active form of JA, Jasmonoyl-isoleucine (JA-Ile) is an essential step for JA signalling responses. In plants, CORONATINE INSENSITIVE 1 (COI1), JASMONATE ZIM-DOMAIN proteins (JAZs) and JAZ-interacting transcription factors have proven to be crucial for the perception of JA signals and the subsequent signal transduction pathway steps [28]. Upon JA-Ile perception, JAZ proteins are specifically bound by COI1, leading to polyubiquitylation and subsequent degradation of JAZ by the 26S proteasome [21]. Degradation of JAZ leads to the expression of jasmonate-responsive genes and derepresses transcription factors such as MYC2 [2, 29, 30]. As repressors for JA signalling, JASMONATE-ZIM-domain (JAZ)

proteins play critical roles in mediating various aspects of the JA response [31]. In addition to the repressor and coreceptor functions of JA signalling, accumulating evidence has shown that JAZ proteins play an integral role in regulating the desensitization of the JA-related pathway, which is essential to preventing uncontrolled JA responses [32].

In tomato, the JAZ family of repressors is composed of an atypical repressor (*SIJAZ13*) and 12 canonical members (*SIJAZ1* to *SIJAZ12*). Individual JAZ genes can exert diverse functions in different plant tissues. As a model plant, *Arabidopsis thaliana* was primarily approved for the JA signalling pathway. Recently, major discoveries about the JA signalling pathway have been made in the model plant (*Arabidopsis thaliana*). Overall, JAZs can play critical roles in the regulation of plant growth and development, and also are essential for controlling pests and diseases [32–35]. However, most of the latest JA-related research has focused on regeneration [19, 36–38]. To date, it has been clarified that JA can induce stem cell activation and regeneration and activate growth after wounding. Nevertheless, the function of JAZ proteins in plant regeneration are needed to be further investigated.

Here, we report that *SIJAZ10* and *SIJAZ11* are involved in leaf senescence and regeneration. Next, we verified that *SIJAZ10*-*SIJAV1*-*SIWRKY51* (JJW) and *SIJAZ11*-*SIJAV1*-*SIWRKY51* (JJW) complexes bind and regulate JA biosynthesis genes. Genetic analysis of overexpression lines demonstrated that *SIJAZ10* and *SIJAZ11* induce self-propagating electrical activity, calcium influx and hormone aggregation after wounding. We also uncovered a new regulatory step in which *SlRbcs-3B* (ribulose biphosphate carboxylase) can stabilize the *SIJAZ11* protein and protect it from degradation of JAZ by the 26S proteasome.

Materials and methods

Plant growth conditions and materials

Tomato (*Solanum lycopersicum* Mill. cv. Ailsa Craig) was selected as wild-type (WT). Tomato seeds were placed on moistened filter paper for 72 h for germination. Tomato plants were grown in a growth chamber at controlled temperature (28°C during the day, 22°C at night) under a 16 h light photoperiod. *Nicotiana benthamiana* plants used for bimolecular fluorescence complementation (BiFC) and dual-luciferase (LUC) assay were grown in the growth chamber with temperature at 26°C and 16 h-8 h, light-dark cycles. All samples were immediately transferred to liquid nitrogen and stored at -80°C until required.

Vector construction and plant transformation

To overexpress *SIJAZ10* and *SIJAZ11*, we amplified the full-length coding sequences (CDSs) of *SIJAZ10* and *SIJAZ11* with *Solanum lycopersicum* Max Super-Fidelity DNA and cloned them into pBI121 vector carrying the cauliflower mosaic virus (CaMV) 35S promoter. To generate CRISPR/Cas9-*SIJAZ10* and CRISPR/Cas9-*SIJAZ11* construct, we inserted two target sites of *SIJAZ10* and *SIJAZ11* (<http://skl.scau.edu.cn/targetdesign>) into the pTX vector with Clone Express II One Step Cloning Kit. By *Agrobacterium* (*Agrobacterium tumefaciens*)-mediated transformation, all constructs were introduced into tomato cv *Ailsa Craig*. Homozygous transgenic plants were used for phenotypic and molecular characterization. The primers used for gene were listed in S1 Table; a standard curve was performed for each pair of specific primers.

Dark treatment for leaf senescence and biochemical assays

Tomato plants were grown in soil for 8 weeks, and the sixth or seventh leaf was detached for dark treatment. The detached leaves were incubated in Petri dishes with two layers of wet filter paper in a dark environment.

TUNEL staining was performed using the DeadEnd Fluorometric TUNEL System. Chlorophyll was extracted in 80% acetone and absorbance measured at 663 and 646 nm for calculation of total chlorophyll content per gram fresh weight. Measurement of malondialdehyde (MDA) was performed with a spectrophotometric assay. Reactive oxygen species (ROS) generation in MRSA was tested with a ROS assay kit. Glutathione (GSH) was measured with the micro reduced glutathione (GSH) assay kit.

RNA isolation and real-time PCR analysis

Total RNA was extracted from various samples with RNAiso plus. First-strand cDNA which was synthesized with a kit. Quantitative reverse-transcription-PCR (qRT-PCR) was performed by Real-Time System. A no-template control was also included in each gene study. All qRT-PCR was performed with three replicates. The primers used for gene were listed in [S2 Table](#); a standard curve was performed for each pair of specific primers.

RNA-sequencing and data analysis

Differentially expressed genes were identified with DESeq2 with a filter threshold of adjusted q-value <0.05 and $|\log_2\text{FoldChange}| > 1$. Cluster Profiler (<http://www.bioconductor.org/packages/release/bioc/html/clusterProfiler.html>) in R package [39] was employed to perform GO and KEGG (<http://www.genome.jp/kegg/>) enrichment analysis [40]. The GO and KEGG enrichment analysis were calculated using hypergeometric distribution with a Q value cutoff of 0.05. Q values obtained by Fisher's exact test were adjusted with FDR for multiple comparisons [41].

Hormone determination analysis

Hormone determination analysis was carried out by high performance liquid chromatography (HPLC). Unsupervised PCA (principal component analysis) was performed by statistics function `prcomp` within R (www.r-project.org). The data was unit variance scaled before unsupervised PCA. The HCA (hierarchical cluster analysis) results of samples and metabolites were presented as heatmaps with dendrograms, while pearson correlation coefficients (PCC) between samples were calculated by the `cor` function in R and presented as only heatmaps. Both HCA and PCC were carried out by R package `pheatmap`. For HCA, normalized signal intensities of metabolites (unit variance scaling) were visualized as a color spectrum.

Ibuprofen (IBU) and 2,3,5-triiodobenzoic acid (TIBA) treatment

For the IBU and TIBA treatment, tomato seeds were firstly germinated in a shaker with temperature set at 28°C and shaker speed 250 r/min for 72 h, then were transferred to ½MS agar medium with or without 100 µM IUB and TIBA in tissue culture flasks for 10 d.

Subcellular localization assay

For subcellular localization, we used *Agrobacterium tumefaciens* strain GV3101 carrying 35S-SIJAZ10-GFP and 35S-SIJAZ11-GFP together with strain p19 (each strain, OD600 = 1.0, 1:1 ratio). At 3d after agroinfiltration, we detected the GFP signals with a confocal microscope. The primers used for gene were listed in [S3 Table](#); a standard curve was performed for each pair of specific primers.

Yeast two-hybrid (Y2H) and Biomolecular Fluorescent Complementation (BiFC) assay

For the Y2H, the Matchmaker GAL4-based two-hybrid system was utilized. Yeast strain Y2H was co-transformed with the specific bait and prey constructs and plated on the SD/Leu/-Trp/-His/-Ade drop-out medium and screened with β -galactosidase.

N. benthamiana leaves were used for BiFC. At 3 days after infiltration, YFP fluorescence was observed with a TCS SP5 confocal spectral microscope imaging system. The primers used for gene were listed in [S4 Table](#); a standard curve was performed for each pair of specific primers.

Pull-down assay

The CDS of *SIJAZ10* and *SIJAZ11* were cloned into pET-28a, and *SIRbcs-3B* into pGEX-4T. These resulted constructs were transformed into *Escherichia coli* BL21 (DE3) to produce recombinant proteins. For pull-down assay, GST-SIJAZ10, GST-SIJAZ11 or GST was incubated with GST Bind Resin at 4°C for 2 h, and then 0.5 mg of purified recombinant protein with His tag was added. The incubation continued for another 6 h, and the beads were washed with pull-down buffer for five times. The bounded proteins were finally eluted, and the pulled down proteins were analyzed by western-blot with the anti-His antibody and anti-GST antibody. The primers used for gene were listed in [S5 Table](#).

Dual-luciferase assay, transcriptional activity and Yeast one hybrid (Y1H)

LUC activity was measured by a dual luciferase assay kit. The *N. benthamiana* leaves were mixed in the PBS 72 h after infiltration. The ratio of LUC to REN was calculated indicate the final transcriptional activity.

Based on the GAL4/UAS-based system, SIJAZ10 and SIJAZ11 transcriptional activity was examined by a dual-LUC reporter assay system.

Y1H experiments were performed according to the Matchmaker Gold Y1H System protocol. The bait plasmids were transformed into the Y1H Gold strain according to the manufacturer's instructions. Aureobasidin A (AbA) was used to screen the minimal inhibitory concentration for the bait strains. The prey plasmid was transformed into a bait yeast strain to determine the DNA-protein interaction by screening them on SD medium with AbA and without leucine. The primers used for gene were listed in [S6 Table](#); a standard curve was performed for each pair of specific primers.

Surface potential recordings

For surface potential recordings, silver electrodes of 0.5 mm diameter were chloridized with HCl (0.1 M), stored at room temperature and rechloridized after several uses. Experiments were conducted in a controlled environment. High impedance amplifier was simultaneously used to record the surface potential at wound positions. The electrode-leaf interface was a drop (10 ml) of 10 mM KCl in 0.5% (w/v) agar placed so that the silver electrode did not contact and damage the cuticle. The ground electrode was placed in the soil. Raw data of surface potentials was acquired with a NI USB 6259 interface, using custom-built Labview-based software.

Detection of intracellular free Ca^{2+} distribution using Fluo-3/AM staining

The 1.0 mM CaCl_2 -treated leaves were probed with Fluo-3/AM to detect the distribution of intracellular free Ca^{2+} ($[\text{Ca}^{2+}]_{\text{cyt}}$) in the cells. The levels of intracellular free Ca^{2+} in leaves were

visualized with a live with excitation wavelength of 488 nm and emission wavelength of 525 nm, and the Ca^{2+} fluorescence intensity was quantified with Image Browser software.

Vitro degradation assays

For in vitro degradation assays, total protein was extracted from the *N. benthamiana* leaves 3 days after injection with native extraction buffer (50 mM Tris-MES, pH8.0, 0.5 M sucrose, 1 mM MgCl_2 , 10 mM EDTA, 5 mM DTT, 1 mM PMSF, and 1* C-complete protease inhibitor). The extracted proteins were then blotted onto nitrocellulose membranes, blocked with nonfat dry milk, and incubated with anti-ACTIN antibody. Protein gel blot pictures were scanned, and the intensity of the images was quantified by ImageJ. The primers used for gene were listed in [S7 Table](#); a standard curve was performed for each pair of specific primers.

Results

JAZ genes respond to the senescence of detached leaves in tomato

To investigate the transcriptional regulation of the senescence of detached leaves in tomato, we treated WT tomato leaves with dark-induced senescence for 8 days. Following the dark-induced senescence treatment, the sequencing results showed a total of 7580 genes (3264 up-regulated genes and 4316 downregulated genes) were significantly different ([Fig 1A](#)). Further analysis of the JAZ family of transcriptome data revealed that many JAZ genes could respond to the senescence of detached leaves ([Fig 1B](#)). Here, *SIJAZ10* and *SIJAZ11* were the two most significantly induced genes by senescence among 13 JAZ. To further validate the transcriptome data, we analysed the senescence expression pattern of *SIJAZ10* and *SIJAZ11* ([Fig 1C](#)). The transcript levels of *SIJAZ10* and *SIJAZ11* always remained at high levels over time. We then constructed a phylogenetic tree of the JAZ family in tomato ([Fig 1D](#)). Homology analysis showed that *SIJAZ10* and *SIJAZ11* shared high homology in protein sequence. Sequence alignments revealed that *SIJAZ10* and *SIJAZ11* share the highest similarities with Arabidopsis *AtJAZ7* and *AtJAZ8*, respectively ([Fig 1E](#)). These observations provided supporting evidence that *SIJAZ10* and *SIJAZ11* presumably played similar roles in the senescence of detached leaves.

SIJAZ10 and SIJAZ11 were involved in the senescence of detached leaves

Because of the high expression levels of *SIJAZ10* and *SIJAZ11* during leaf ageing, we generated knockout lines by the CRISPR/Cas9 technique and overexpression lines by the CaMV 35S promoter. From the transgenic progeny, we selected two homozygous knockout lines (*sljaz10* and *sljaz11* one for each) ([Fig 1F](#)) and three overexpression lines with high expression levels of *SIJAZ10* and *SIJAZ11*, respectively, for phenotypic analysis (*SIJAZ10-OE-11*, *SIJAZ10-OE-18*, *SIJAZ10-OE-21*, *SIJAZ11-OE-3*, *SIJAZ11-OE-6* and *SIJAZ10-OE-9*) ([Fig 1G](#)). Compared with the WT ([Fig 2A](#)), *sljaz10* and *sljaz11* showed obvious yellowing at approximately the same time (8 d dark treatment). In contrast to the knockout lines, *SIJAZ10-OE* leaves displayed little chlorotic symptoms and *SIJAZ11-OE* leaves almost did not display chlorosis, while WT leaves showed obvious chlorotic symptoms in the ageing phase (8 d dark treatment).

To further substantiate the above results, we performed biochemical and qRT-PCR analysis of the samples with dark-induced leaf senescence. TUNEL assay showed that the ratios of dead to live cells of *sljaz10* and *sljaz11* indistinguishable from the WT were observed and the cell survival rate of *SIJAZ10-OE* and *SIJAZ11-OE* was higher than the WT ([Fig 2B](#)). Measurement of chlorophyll content showed that chlorophyll loss was much slower in the leaves of the overexpression lines (*SIJAZ10-OE* and *SIJAZ11-OE*) than in the wild type and in knockout lines

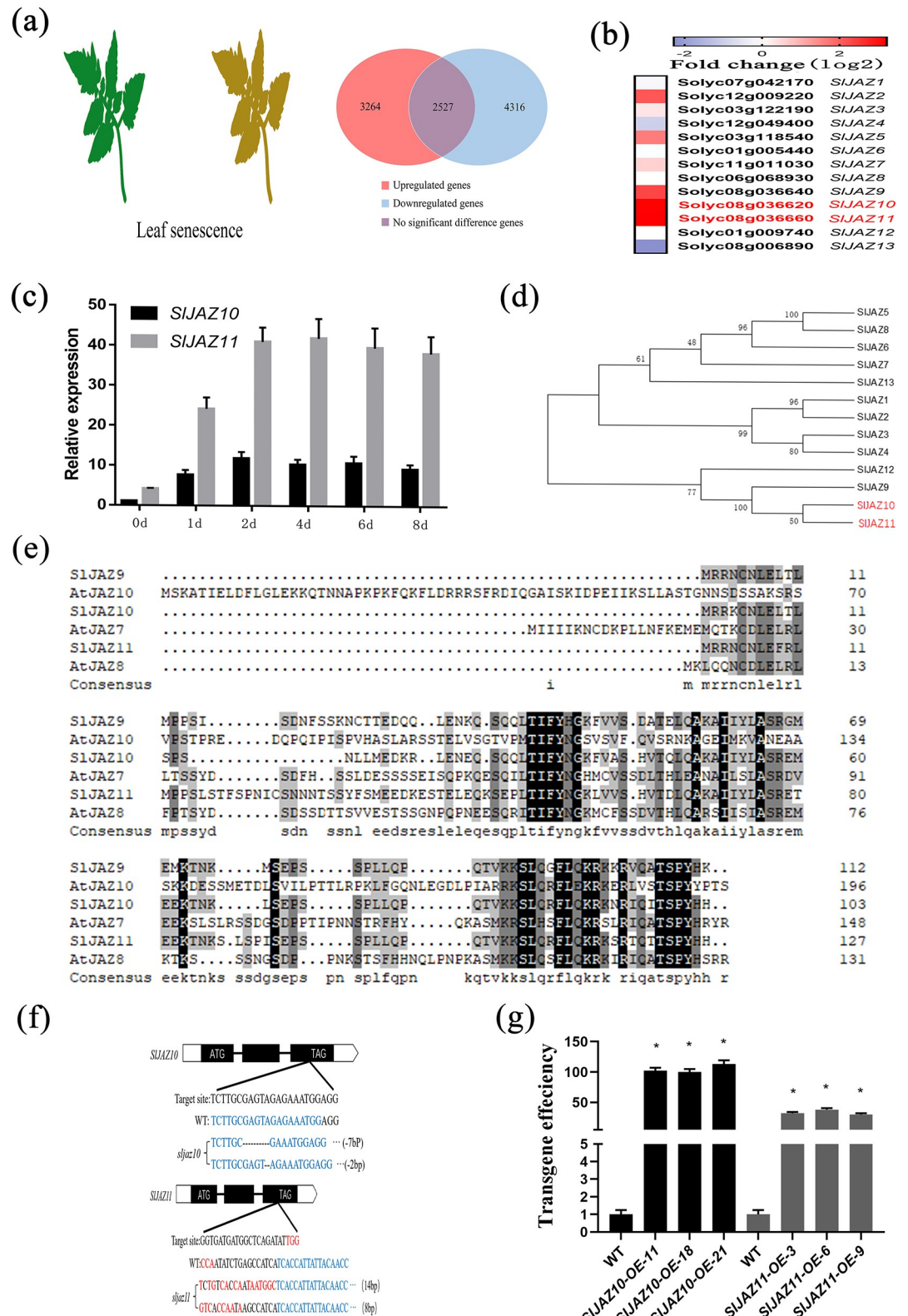


Fig 1. Expression of *SIJAZ10* and *SIJAZ11* is induced after dark treatment. (a) Distribution of genes upregulated or downregulated by dark treatment in the wild-type. (b) Expression of representative SIJAZ genes during aging. The fold-change in the average expression (log₂ scale) of each gene is shown. WT samples were taken 8 days after dark treatment.

Three independent biological samples were used. (c) The relative expression level of *SIJAZ10* and *SIJAZ11* during aging. (d) Phylogenetic analysis of JAZ proteins in tomato. (e) Amino acid sequence alignment of *SIJAZ10* and *SIJAZ11* homologues. (f) *sljaz10^{ko}* (CRISPR/Cas9-*SIJAZ10*) and *sljaz11^{ko}* (CRISPR/Cas9-*SIJAZ11*) alleles identified from the T1 mutants of tomato. (g) The *SIJAZ10*-overexpressing (OE) and *SIJAZ11*-overexpressing (OE) lines. The tissue examined was mature leaf.

<https://doi.org/10.1371/journal.pgen.1010285.g001>

(*sljaz10* and *sljaz11*) under dark treatment (Fig 2C). Correspondingly, MDA content was significantly lower in both overexpression lines than in the WT and knockout lines (Fig 2D). Given that the accumulation of mitochondrial ROS and GSH has been linked to cellular senescence [42], we performed measurements on all samples. After dark treatment, the ROS content of the two overexpression lines was significantly lower than that in the WT and knockout lines (Fig 2E), and the GSH content in the overexpression lines greatly increased than that in the WT and knockout lines (Fig 2F). The survival rate results were consistent with the biochemical results reported above (S1 Fig). To verify the accuracy of the biochemical indicators, eight transcriptional regulatory genes (*SIGLK1*, *SISGR1*, *SITAS14*, *SIGME2*, *SISAG12*, *SISAG15*, *SISOD* and *SIGST*) involved in the physiological indices mentioned above were selected for quantification. As anticipated, these consequences of quantitative analysis were consistent with the biochemical parameters during leaf ageing (Fig 2G–2N). In summary, these results suggest that knockout of *SIJAZ10* or *SIJAZ11* did not affect the antiaging effect of the transgenic plant leaves, but it could enhance the antiaging effect by overexpressing *SIJAZ10* or *SIJAZ11*, respectively.

***SIJAZ10* and *SIJAZ11* regulate regeneration through JA signalling**

To probe the antiaging limits of *SIJAZ10-OE* and *SIJAZ11-OE* transgenic lines, we prolonged the dark-treatment from 8 to 14 days. Although many transgenic line leaves began to exhibit senescence, they did better than WT leaves. Quite unexpectedly, some stay-green leaves formed calli and generated roots at the petiole (Fig 3A). For statistical analysis, both the rooting rate of *sljaz10^{ko}* and *SIJAZ10-OE* transgenic plants was indistinguishable from WT, but overexpression of *SIJAZ11* could dramatically promote rooting (Fig 3B).

Subsequently, we performed transcriptome sequencing analysis of dark-treated leaf samples after 8 days. Compared with wild-type leaves, differential gene expression analysis revealed that 4791 and 5732 genes were affected in *SIJAZ10-OE* and *SIJAZ11-OE* transgenic lines, respectively, during dark-treatment (S2A Fig). The DEGs of the two transgenic plants were further refined through Gene Ontology (GO) enrichment and KEGG pathway enrichment analyses (S2B and S2C Fig), and the results showed that *SIJAZ10* and *SIJAZ11* could coordinate primary and secondary metabolites to resist to senescence. A large number of DEGs associated with the IAA and JA signalling pathways were identified in both *SIJAZ10-OE* and *SIJAZ11-OE* lines (Fig 3C and 3D). After measuring the JA and IAA contents of untreated samples, we revealed that only the JA content of *SIJAZ11-OE* was significantly upregulated (Fig 3E). The results of hormone metabolism analysis indicated that only JA and JA-Ile contents were upregulated significantly in the *SIJAZ11-OE* transgenic lines after dark-treatment (Fig 3F). To further validate the effects of hormones on the *sljaz10*, *SIJAZ10-OE*, *sljaz11* and *SIJAZ11-OE* transgenic lines, we further treated seedlings with JA biosynthetic inhibitor ibuprofen (IBU) and auxin transport inhibitor (TIBA) (S3 Fig). When compared with the wild-type, all transgenic lines (*sljaz10*, *SIJAZ10-OE*, *sljaz11* and *SIJAZ11-OE*) were less sensitive to IBU and were not significantly different with TIBA treatment. The *SIJAZ11-OE* transgenic lines showed better root development than *SIJAZ10-OE* transgenic lines with IBU treatment. The joint analysis of hormone and transcriptomics data and its responsiveness to JA suggested that the JA signalling pathway was a critical factor in antiaging and regeneration.

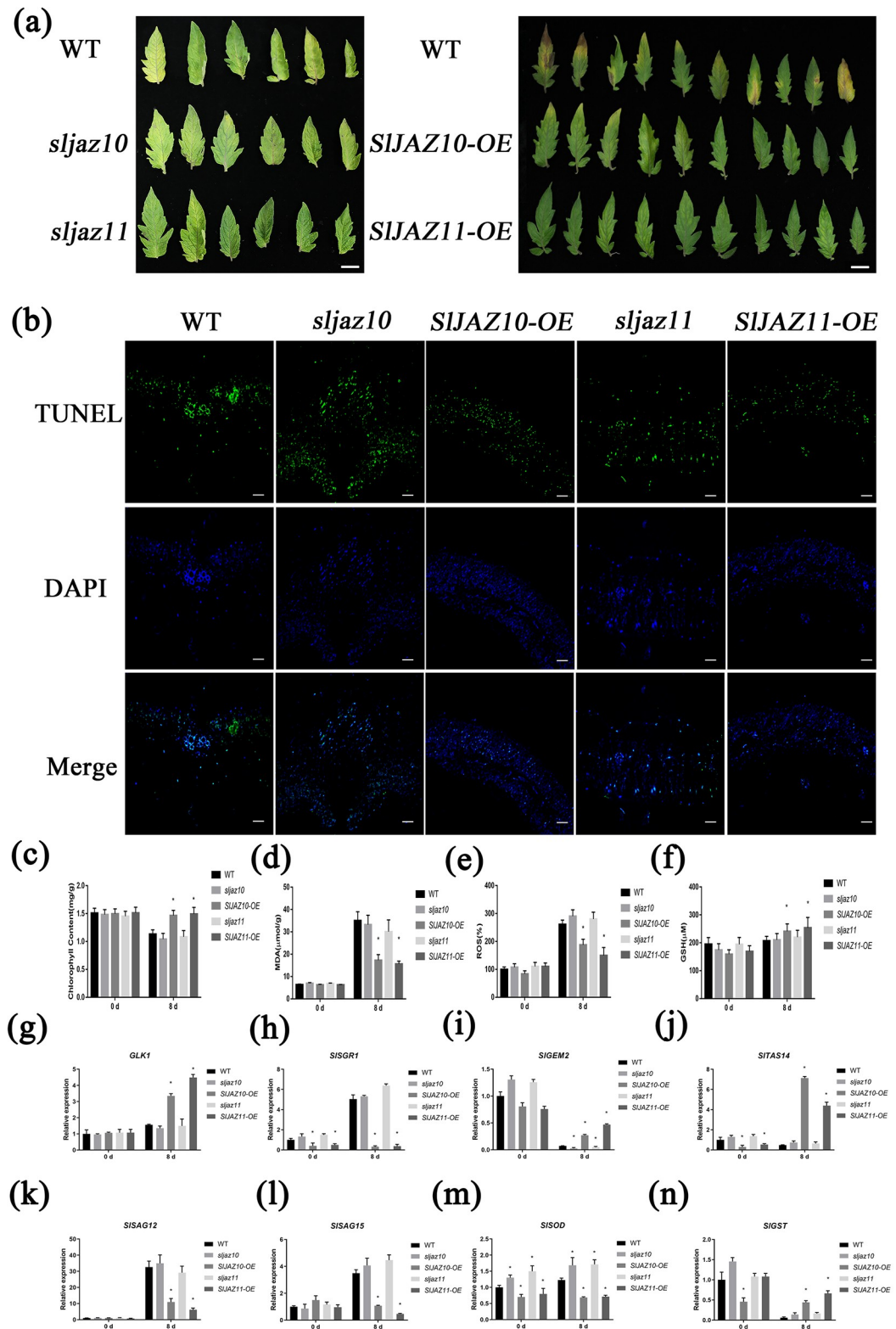


Fig 2. Physiological analyses of the mature leaves in tomato wild-type (WT), knockdown lines and overexpression lines after 8 days dark treatment. (a) Mature leaves of the wild type, knock-out, and overexpression lines under dark treatment, incubated with wetted filter paper in dark conditions for 8d, and photographed. (b) Cell death was detected using the TUNEL assay. Representative images show TUNEL staining results (blue, DAPI; green, TUNEL). (c-f) Contents of chlorophyll, MDA, ROS and GSH in the leaves of the

WT, *sljaz10*, *SIJAZ10*-OE, *sljaz11* and *SIJAZ11*-OE after dark treatment. (g-n) Relative expression of eight genes related to the above physiological phenotypes. All data are means (\pm SE) of three independent biological replicates. * $P < 0.01$ (significant difference between mutants and WT according to Student's t-test).

<https://doi.org/10.1371/journal.pgen.1010285.g002>

JJW (SIJAZ10-SIJAV1-SIWRKY51 or SIJAZ11-SIJAV1-SIWRKY51) binds and represses JA biosynthesis gene (*SIAOC*)

In previous studies, JAV1, JAZ8 and WRKY51 were shown to form a corepressor complex to bind and repress JA biosynthesis genes in *Arabidopsis* [37]. Y2H screening showed that SIJAV1 interacts with SIJAZ10 and SIJAZ11 (Fig 4A). However, toxicity testing indicated that the full-length SIWRKY51 protein caused toxic effects in the yeast host cell, so there was no Y2H assay for SIWRKY51. The subcellular localization assay showed that SIJAZ10 and SIJAZ11 were associated with the nucleus and membrane (Fig 4B). Further BIFC and Co-IP assays detected physical interactions among SIJAZs (SIJAZ10 or SIJAZ11), SIJAV1, and SIWRKY51 in vivo (Figs 4C and S4).

In *Arabidopsis*, the JAV1-JAZ8-WRKY51 complex directly bound to the W-box of the AOS promoter (JA biosynthesis gene) [43]. Subsequent analysis showed that the W-box motif was present in the promoters of *SIAOC* (JA biosynthesis gene) and *SIAOS* (JA biosynthesis gene). For this purpose, we used specific primers surrounding the W-box of the *SIAOC* and *SIAOS* promoters for the Y1H assay (Figs 4D and S5). Unexpectedly, the SIJAV1 and SIWRKY51 proteins could bind to the promoter of *SIAOC* and W-box but not to the promoter of *SIAOS*, while SIJAZ10 and SIJAZ11 could not bind to the W-box motif in the promoter of *SIAOC* and *SIAOS*.

Subsequently, transcriptional activity experiments indicated that the SIJAZ10 and SIJAZ11 proteins had transcriptional repressive activity (Fig 4E). The JJW complex did not enhance the suppression of SIJAZ10 and SIJAZ11 (S6 Fig). To evaluate the effect of SIJAZ10, SIJAZ11, SIJAV1 and SIWRKY51 on *SIAOC* and *SIAOS* expression, the promoters of *SIAOC* and *SIAOS* were fused with the luciferase gene to generate the reporters, whereas SIJAZ10, SIJAZ11, SIJAV1 and SIWRKY51 driven by the CaMV 35S promoter were used as effectors (Figs 4F and S7A). As shown, both individual proteins in all reporters and the JJW protein complex significantly repressed the activity of *SIAOC_{pro}-LUC*. However, none of the effectors regulated the activity of *SIAOS_{pro}-LUC* (S7B Fig). Consistent with the dual-luciferase assay, quantitative PCR analysis showed that only *SIJAZ11* could regulate the expression of *SIAOC* (S7C Fig). Enhanced binding of JJW was observed upon mutation of the W-box (Fig 4G). Interestingly, although both of the *SIAOC* and *SIAOS* promoters contain W-box motifs, only the promoter of *SIAOC* was regulated by JJW.

Injury-triggered regeneration in transgenic tomato plants

Because many regulators of electrical signals and calcium (Ca^{2+}) waves were heavily enriched in the transcriptome data of dark-treated samples (Table 1), we next focused our work on the changes in electrical signals and Ca^{2+} waves after wounding. The surface potential from the proximal wound area to the proximal wound area was measured from damage initiation to 20 min. The results of wound-activated surface potential changes (WASPs) of variable amplitude are shown in Fig 5A. For the periods of time after wounding, the electrical signal of WT was first transmitted from the distal ends to the wound and then transmitted to the distal ends. For *SIJAZ10*, the electrical signal of both knockdown and overexpression transgenic lines was virtually unchanged after wounding. However, the electrical signal of the *sljaz10* transgenic line consistently transported away from the wound while the electrical signal of the *SIJAZ11*-OE

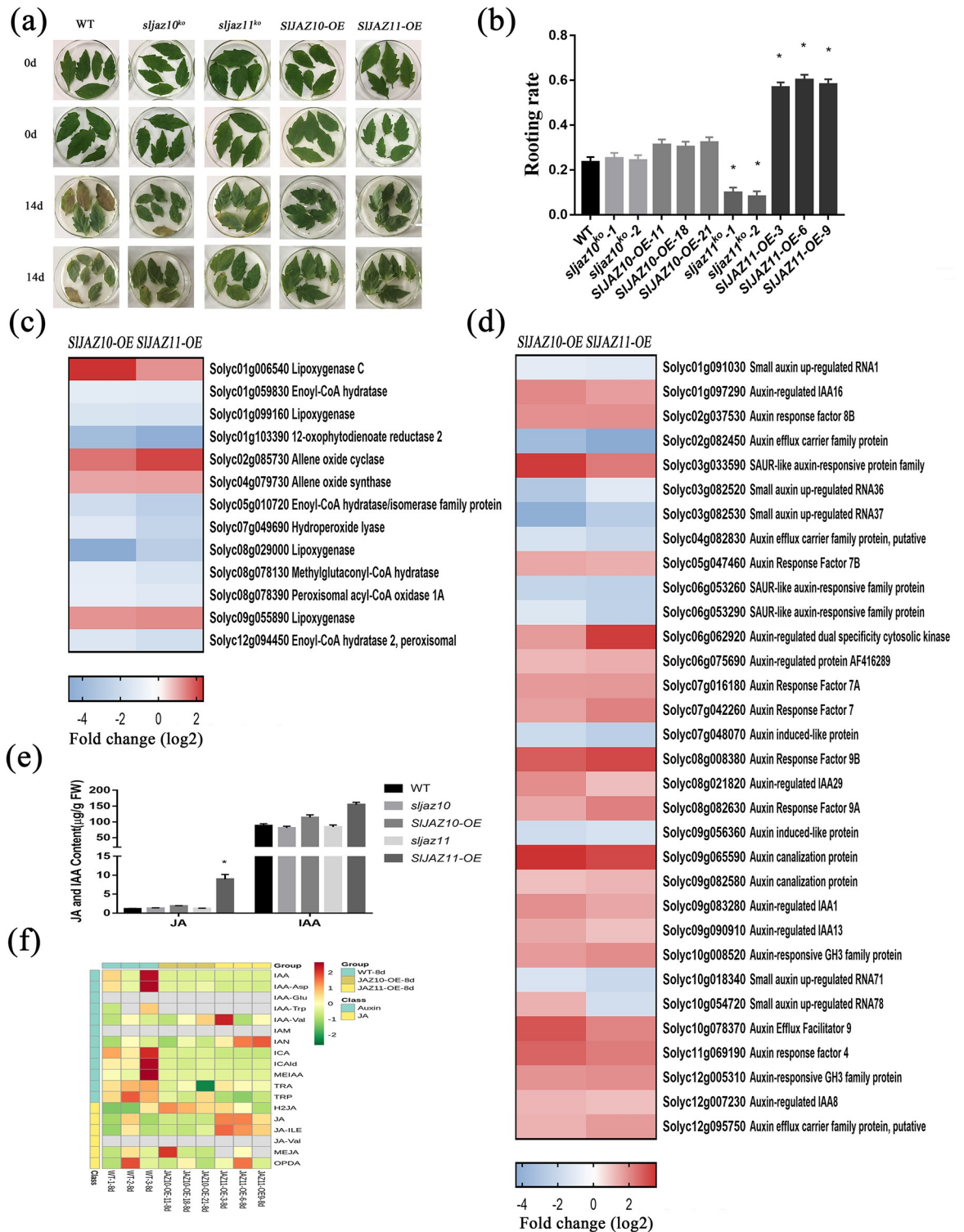


Fig 3. *SIJAZ10* and *SIJAZ11* regulate JA and IAA signaling in dark-induced senescence. (a) Mature leaves of the wild type and transgenic lines under dark treatment, incubated with wetted filter paper in dark conditions for 14d, and photographed. (b) The rooting rate of the wild type and transgenic lines under 14d dark treatment. * $P < 0.01$ (significant difference between mutants and WT according to Student's t-test). (c) Expression of JA-responsive related genes in the RNA-seq experiments. The fold-change in the average expression (log₂ scale) of each gene is shown. (d) Expression of IAA-responsive related genes in the RNA-seq experiments. The fold-change in the average expression (log₂ scale) of each gene is shown. (e) JA content and IAA content of senescent leaves. (f) Heatmaps of hormone metabolism. The heat maps represent the log₂ fold changes of DEGs related to hormone metabolisms.

<https://doi.org/10.1371/journal.pgen.1010285.g003>

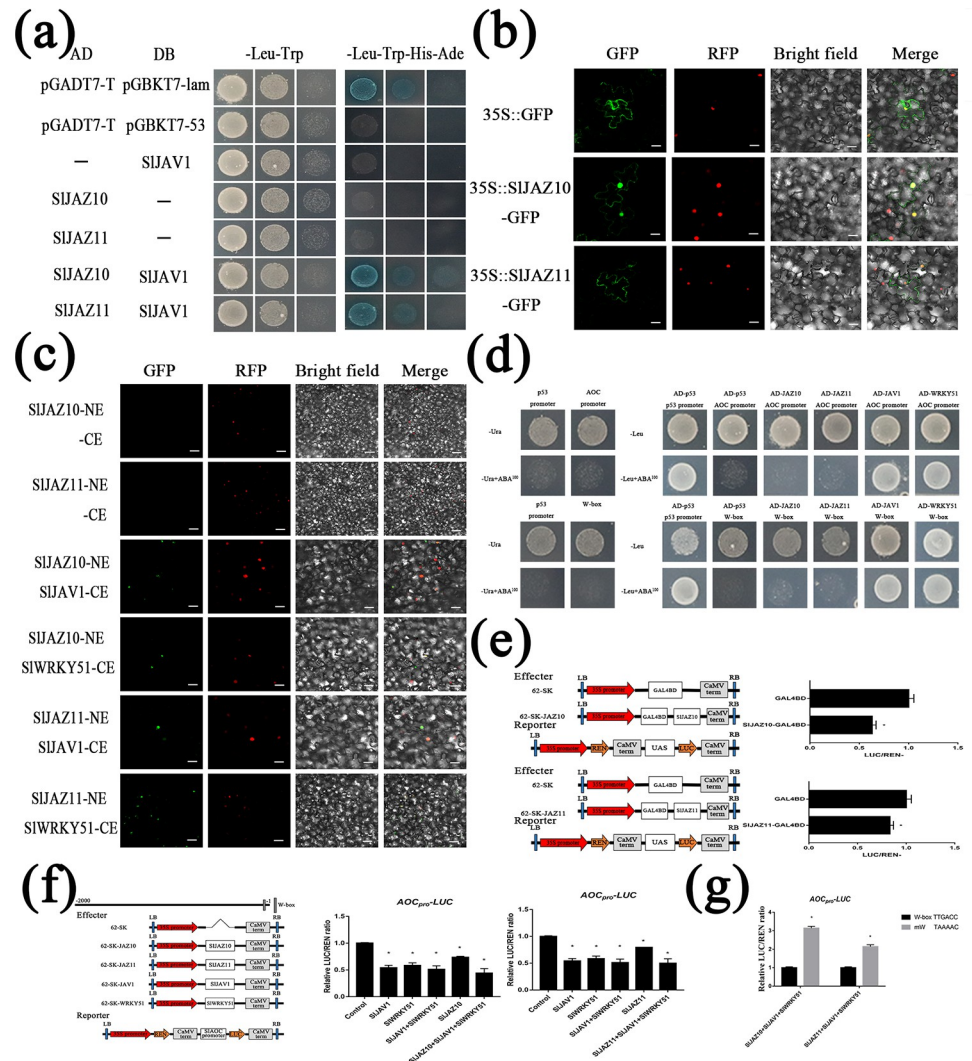


Fig 4. The JJW (SIJAZ10-SIJAV1-SIWRKY51 or SIJAZ10-SIJAV1-SIWRKY51). (a) Y2H assay shows that SIJAV1 interacts with SIJAZ10 and SIJAZ11. (b) Subcellular localization of SIJAZ10 and SIJAZ11 in the epidermal cells of *N. benthamiana* leaves. Bars = 40µm. (c) BiFC assay confirms the interactions among SIJAZ10, SIJAZ11, SIJAV1 and SIWRKY51 in *N. benthamiana* leaves. (d) Y1H assay shows the transcriptional binding activity of SIJAZ10 and SIWRKY51 with *SIAOC* promoter. (e) Transient transcriptional activation assays show that SIJAZ10 and SIJAZ11 have transcriptional repression activity. (f) SIJAZ10-SIJAV1-SIWRKY51 and SIJAZ11-SIJAV1-SIWRKY51 complex effectively suppresses the expression of *SIAOC*_{Pro}-LUC in *N. benthamiana* transient expression assay. Relative ratio of LUC/REN are means ± SEM (n≥6); *p < 0. and *p < 0.05; Student's t test. (g) Relative expression of the luciferase gene (LUC) driven by the 130bp upstream fragment of the *SIAOC* promoter, with the W-box intact or mutated.

<https://doi.org/10.1371/journal.pgen.1010285.g004>

transgenic line throughout converged towards the wound. Similar to the WSAP results after wounding (Fig 5B), the wave of Ca²⁺ movement in WT, *sljaz10* and *SIJAZ10-OE* was disorganized, while the movement of Ca²⁺ in the *sljaz11* transgenic line moved from the wound to the distal ends and in the *SIJAZ11-OE* transgenic line, it converged towards the wound.

In *Arabidopsis*, the regulation of JA and IAA was accomplished by the rapid response electrical signal and Ca²⁺ wave [44, 45]. Therefore, we measured the changes in the JA and IAA contents at the two ends of the wound (Fig 5C). Following injury, the total content of JA and IAA showed a gradually decreasing trend in all samples. An unexpected observation was that the relative content of JA and IAA of the two ends of the wound had a certain regularity in its

Table 1. Differential genes expression analysis.

#	Locus Identifier	logFC (SIJAZ10)	PValue (SIJAZ10)	LogFC (SIJAZ11)	PValue (SIJAZ11)	Annotation
1	Solyc01g008130	-1.7671874	2.02E-43	-2.975199912	2.31E-82	Electron protein, putative (Protein of unknown function, DUF547)
2	Solyc02g089980	-	-	1.250324751	3.30E-18	Electron transporter, putative (Protein of unknown function, DUF547)
3	Solyc04g082970	-	-	2.12014617	1.42E-86	Electron protein, putative (Protein of unknown function, DUF547)
4	Solyc08g078520	1.757863942	3.91E-07	1.716670736	3.13E-06	Electron transporter, putative (Protein of unknown function, DUF547)
5	Solyc09g089880	-1.5977942	2.50E-67	-2.385733953	3.34E-120	Electron transfer flavoprotein beta-subunit, putative
6	Solyc12g005200	-2.902997529	3.74E-283	-3.455028482	5.92E-318	Electron transfer flavoprotein alpha subunit
7	Solyc01g007170	1.847217662	1.44E-05	2.116576732	3.83E-06	C2 calcium/lipid-binding plant phosphoribosyl transferase family protein
8	Solyc01g065500	1.811816639	3.01E-33	2.64713281	4.25E-75	C2 calcium/lipid-binding plant phosphoribosyl transferase family protein
9	Solyc01g073710	-1.133565739	1.34E-14	-1.987680422	4.56E-33	Calcium-binding EF hand family protein
10	Solyc01g091465	3.366723725	2.28E-08	3.77719715	8.27E-11	Calcium-binding EF-hand
11	Solyc01g097420	-2.079749473	7.31E-14	-3.412797764	1.55E-21	Calcium-transporting ATPase
12	Solyc01g099385	-2.203688611	1.92E-10	-1.680613943	7.33E-07	Calcium-dependent lipid-binding (Ca LB domain) family protein
13	Solyc01g104150	1.414469094	1.25E-04	2.209209922	5.25E-10	Calcium ion-binding protein
14	Solyc01g108190	-1.289510585	9.15E-58	-2.354040652	1.85E-153	Calcium-binding EF-hand
15	Solyc02g065555	-1.672617962	5.53E-75	-1.647949923	2.36E-78	Calcium uniporter, mitochondrial
16	Solyc02g079520	2.646693288	1.12E-63	3.562434818	2.66E-159	Calcium-binding EF-hand protein
17	Solyc02g083850	-1.80201821	4.92E-60	-2.760931591	1.53E-88	Calcium-dependent protein kinase
18	Solyc02g088090	1.014703362	5.13E-23	2.153781727	3.11E-111	Calcium-binding EF-hand
19	Solyc02g090560	2.607959043	1.63E-16	2.162216007	9.53E-09	Calcium-transporting ATPase
20	Solyc03g006260	3.540268625	2.08E-24	2.680131648	8.61E-09	Calcium-binding EF-hand
21	Solyc03g044960	-5.423833409	1.42E-209	-7.181839469	8.39E-213	Calcium uniporter protein, mitochondrial
22	Solyc04g007800	1.800590518	2.16E-07	1.514884396	1.92E-04	Calcium-dependent lipid-binding (Ca LB domain) family protein
23	Solyc04g015070	1.927481861	3.04E-17	2.374922391	1.31E-27	Calcium-dependent lipid-binding (Ca LB domain) family protein
24	Solyc04g058160	-1.406953835	1.87E-20	-2.984968019	5.16E-46	Calcium-binding protein
25	Solyc04g058170	-3.527497763	1.03E-29	-3.500188831	4.16E-25	Calcium-binding protein
26	Solyc07g045210	1.248666809	2.56E-38	1.388869303	3.84E-47	Calcium ion-binding protein
27	Solyc08g008020	1.627514206	6.48E-08	2.564625232	5.85E-18	C2 calcium/lipid-binding plant phosphoribosyl transferase family protein
28	Solyc09g007860	-3.061286993	1.67E-34	-3.675206534	9.11E-38	Calcium-dependent lipid-binding (Ca LB domain) family protein
29	Solyc10g006740	2.907308454	6.29E-10	3.229458205	5.95E-12	Calcium-binding family protein
30	Solyc10g050060	-1.638049538	1.24E-72	-1.503471306	1.47E-62	Calcium-dependent lipid-binding (Ca LB domain) family protein
31	Solyc10g074570	-1.575154962	6.59E-72	-2.027645716	3.37E-120	Calcium-dependent protein kinase family protein
32	Solyc10g078680	4.587793038	2.39E-66	4.803329662	6.82E-76	C2 calcium/lipid-binding and GRAM domain protein
33	Solyc10g080420	1.101188016	8.14E-34	1.498154783	1.77E-64	C2 calcium/lipid-binding and GRAM domain protein
34	Solyc11g018610	-1.157052799	4.19E-12	-1.019775783	5.83E-09	Calcium-dependent protein kinase
35	Solyc11g022460	1.194261168	1.20E-26	1.488195894	3.26E-36	C2 calcium/lipid-binding plant phosphoribosyl transferase family protein
36	Solyc11g068460	-1.915436535	1.12E-78	-1.106358978	6.89E-34	Ef-hand calcium binding protein, putative
37	Solyc12g011420	-1.119432794	2.12E-12	-2.4207635	4.94E-33	Calcium-dependent lipid-binding domain protein
38	Solyc12g014110	1.287057008	1.45E-32	1.796354305	7.64E-66	Sodium/calcium exchanger family protein / calcium-binding EF hand family protein
39	Solyc12g088840	2.54541436	7.85E-82	2.056328816	3.20E-34	Calcium-binding EF-hand family protein, putative

<https://doi.org/10.1371/journal.pgen.1010285.t001>

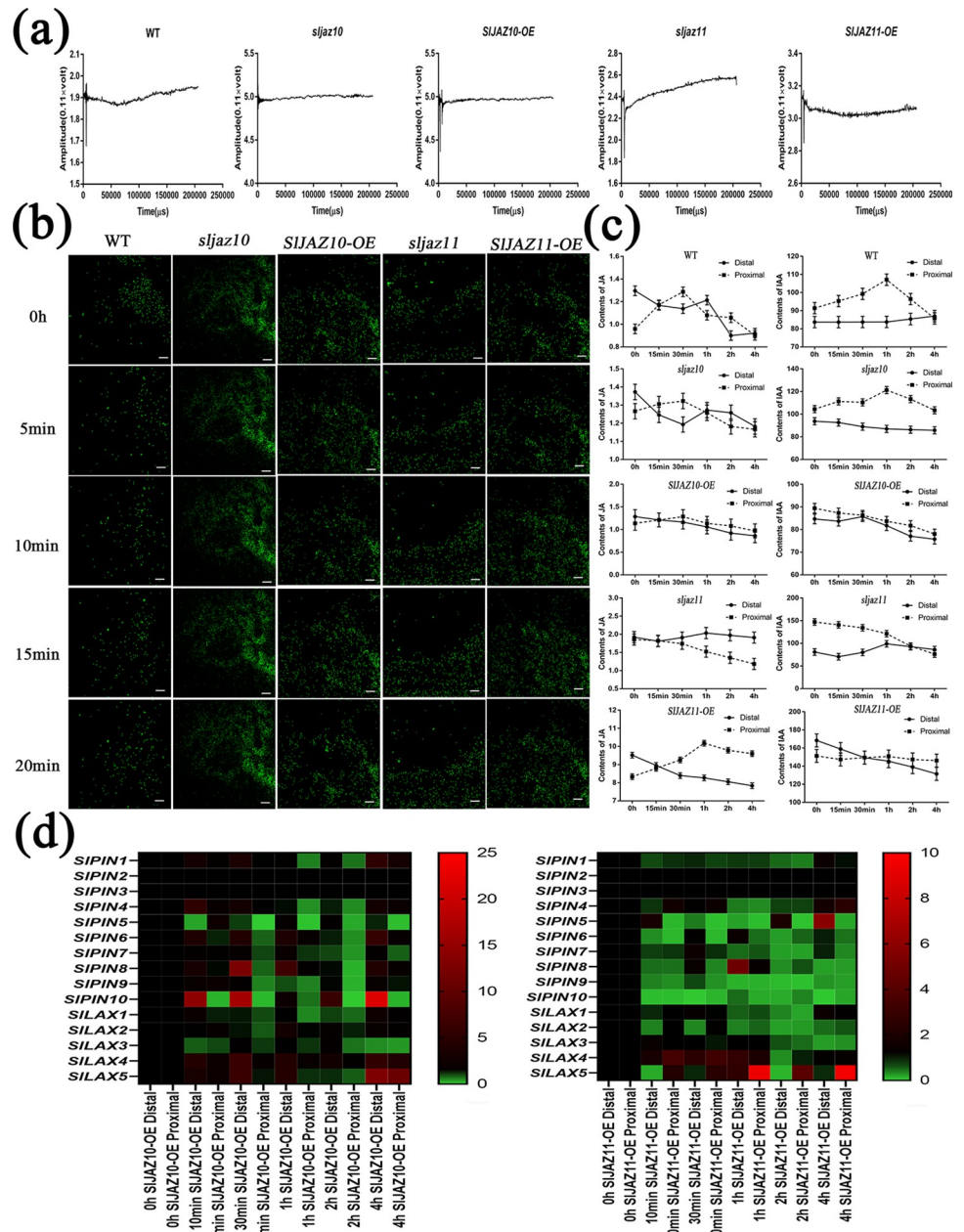


Fig 5. Changes in electrical signals, calcium signals and hormone transports during injury-induced regeneration. (a) Typical WASPs in wild type (WT), *sljaz10*, *SIJAZ10-OE*, *sljaz11* and *SIJAZ11-OE* after wounding leaves. (b) Confocal image of $[Ca^{2+}]_{cyt}$ in WT, *sljaz10*, *SIJAZ10-OE*, *sljaz11* and *SIJAZ11-OE* after wounding leaves. (c) Relative contents of JA and IAA at both ends of the wounding leaves. (d) Heatmap of auxin transport unigenes at both ends of the wounding leaves.

<https://doi.org/10.1371/journal.pgen.1010285.g005>

spread. Immediately after injury, the contents of JA and IAA (WT, *sljaz10* and *SIJAZ10-OE*) were actively transported into the approximate wound boundary, and they were transported further away from the wound after a while. In the *sljaz11* transgenic line, JA and IAA were slowly transported from the proximal ends to the distal ends. In contrast to the other transgenic, JA and IAA were concentrated close to the wound in the *SIJAZ11-OE* transgenic line.

By qRT-PCR, we found that many auxin transport-related genes displayed significant changes at the two ends of the wound (Fig 5D). In *SIJAZ10-OE* and *SIJAZ11-OE* transgenic lines, these auxin transport-related genes were induced to respond to injury upon mechanical wounding. Overall, different from the regulation of *SIJAZ10* after wounding, the regulation of *SIJAZ11* was performed towards the wound ends.

Ca²⁺ and SIRbcs-3B control JJW-regulated JA biosynthesis for regeneration

The calcium ions efficiently degraded JAZ-JAV-WRKY protein complexes by phosphorylation of JAV1 [37]. Given the injury experiment results, we investigated the effects of Ca²⁺ on JJW activity (Fig 6A). Coexpression of Ca²⁺ and SIJAV1 obviously promoted *SIAOC_{pro}-LUC* expression compared to SIJAV1 alone. Moreover, the repression of SIJVA1-SIWRKY51 complex activity was abolished by Ca²⁺. Interestingly, after the addition of Ca²⁺, the transcriptional function of SIJAZ11 or the SIJAZ11-SIJAV1-SIWRKY51 complex transforms the repression to activation of *SIAOC*. However, Ca²⁺ did not change the repression of the SIJAZ10 and SIJAZ10-SIJAV1-SIWRKY51 complex. All correlation changes occurred only for *SIAOC* but not for *SIAOS* (S8 Fig).

To gain further insights into the molecular functions of SIJAZ10 and SIJAZ11, we searched for interacting proteins by yeast two-hybrid screening. SIRbcs-3B (ribulose biphosphate carboxylase small chain), a photosynthesis gene, was identified by yeast two-hybrid screening (Fig 6B). In agreement with the literature report [46], the analysis of subcellular localization showed that SIRbcs-3B was localized in the nucleus (Fig 6C). The interaction in the Y2H assay was further validated by BiFC (Fig 6D) and pull-down assays (Fig 6E).

To figure out the function of SIRbcs-3B in JA biosynthesis for regeneration, we focused on its regulation of JJW complexes. The experiments with a dual-luciferase-reporter indicated that SIRbcs-3B may not only drastically induce the expression of *SIAOC* promoters but also switch the activity of SIJAZ11-SIJAV1-SIWRKY51 from inhibition to promotion (Fig 6F). Real-time PCR of senescent samples revealed that the expression of *SIJAV1*, *SIWRKY51* and *SIRbcs-3B* was induced to varying degrees by *SIJAZ10* and *SIJAZ11* during leaf senescence (Fig 6G). From the above protein experiments, we also found that SIJAZ11 proteins might be degraded rapidly. In vitro protein degradation assays (Fig 6H) demonstrated that the SIJAZ11 protein was indeed susceptible to degradation. SIRbcs-3B might promote the stabilization of SIJAZ11 protein within a certain period of time. Collectively, Ca²⁺ and SIRbcs-3B could alter the regulatory function of JJW to regulate regeneration.

Discussion

Senescence is a multifactorial process integrating hormonal and molecular perturbations. JA plays an important role in plant senescence and defence [47]. Both natural and dark-induced senescence could lead to high JA levels [48]. By suppressing transcription factors, JAZs maintain JA at low levels to repress the expression of JA-responsive genes [49]. However, JAZs are rapidly degraded upon high JA levels, which can release and trigger JA signalling pathway activation [50]. In *Arabidopsis*, JAZ7-mediated MYC-regulated indole-GS genes are involved in leaf senescence [6], and JAZ8 is a component of the inhibitory JA signalling pathway that could lead to the inhibition of plant growth and reduce plant defence [51]. Our phenotypic observations of transgenic lines are consistent with these data and further support the regulatory mechanisms of leaf senescence through the JAZ signalling pathway. The *SIJAZ10* and *SIJAZ11* overexpression transgenic lines strongly enhanced the ability to resist dark-induced senescence (Fig 2) by JA-mediated signalling pathways (Fig 3). We found that *SIJAZ10* and *SIJAZ11* repressed ageing related genes to negatively regulate leaf senescence, agreeing with

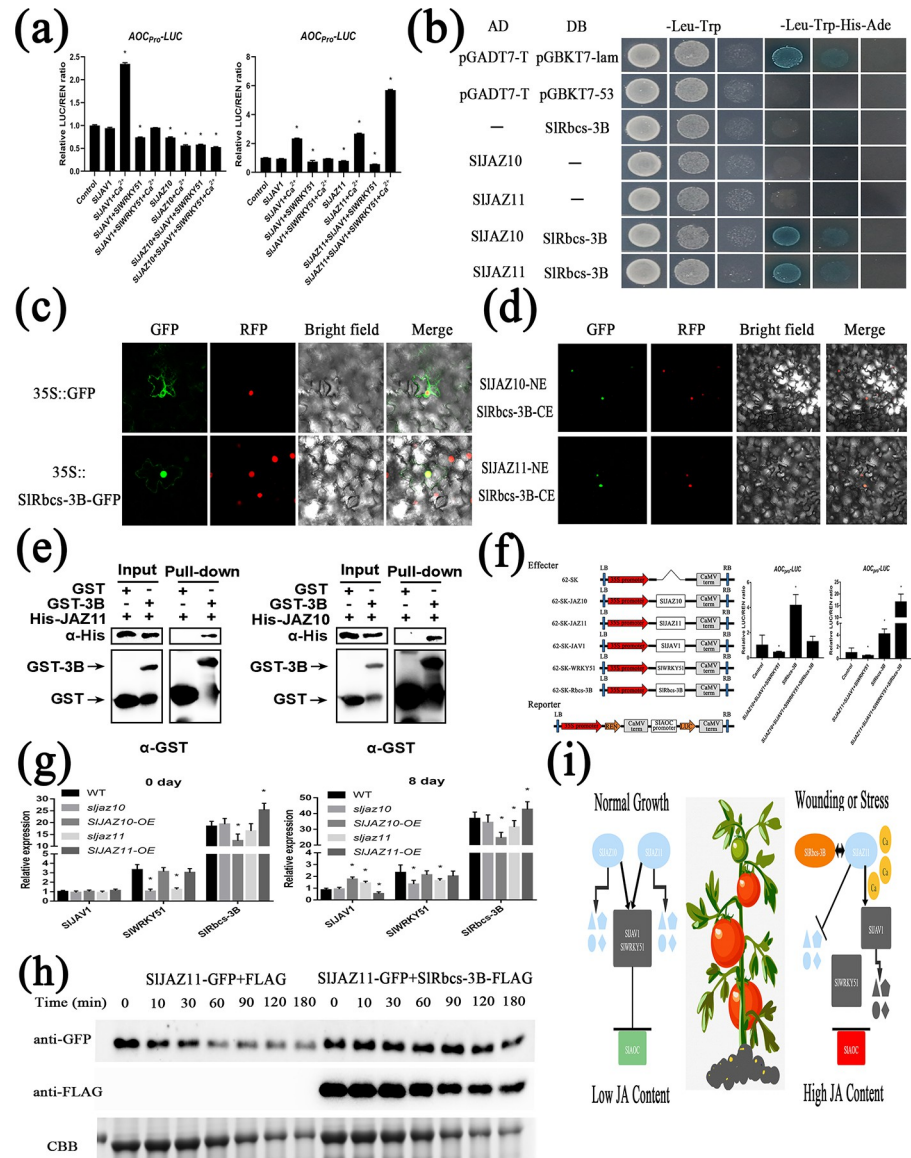


Fig 6. Ca^{2+} and SIRbcs-3B inactivates JJW Complex. (a) Ca^{2+} alter transcriptional repression of SIJAZ10-SIJAV1-SIWRKY51 and SIJAZ11-SIJAV1-SIWRKY51 complex on the *SIAOC_{Pro}-LUC* expression. Relative ratio of LUC/REN are means \pm SEM ($n \geq 6$); * $p < 0.01$; Student's t test. (b) Y2H assay shows that SIRbcs-3B interacts with SIJAZ10 and SIJAZ11. (c) Subcellular localization of SIRbcs-3B in the epidermal cells of *N. benthamiana* leaves. Bars = 40 μ m. (d) BiFC assay confirms the interactions among SIJAZ10, SIJAZ11, and SIRbcs-3B in *N. benthamiana* leaves. (e) The interaction of His-SIJAZ10 and His-SIJAZ11 with GST-SIRbcs-3B detected by the pull-down assay. GST-SIRbcs-3B was used as bait, and pull-down of His-SIJAZ10 and His-SIJAZ11 was detected by anti-His antibody. (f) SIRbcs-3B alters transcriptional repression of SIJAZ11-SIJAV1-SIWRKY51 complex on the *SIAOC_{Pro}-LUC* expression. Relative ratio of LUC/REN are means \pm SEM ($n \geq 6$); * $p < 0$; Student's t test. (g) qRT-PCR analysis of transcript levels of *SIJAV1*, *SIWRKY51* and *SIRbcs-3B* in dark-treatment leaves of WT, *sljaz10*, *SIJAZ10-OE*, *sljaz11* and *SIJAZ11-OE* plants. Data are means \pm SEM ($n \geq 3$); * $p < 0.01$; Student's t test. (h) SIRbcs-3B promotes maintenance the stabilization of SIJAZ11 proteins in vivo. Proteins were extracted from *N. benthamiana* leaves transiently expressing SIJAZ11-GFP or SIRbcs-3B-Flag alone. Extracts containing SIRbcs-3B-Flag were incubated with SIJAZ11-GFP or GFP extracts for different times. Degradation of SIJAZ11-GFP was detected by anti-GFP antibody. An equal amount of SIRbcs-3B-Flag or Flag was detected by anti-Flag antibody. The equal amount of protein stained by CBB was used as a loading control. (i) A simplified model for injury-triggered JA biosynthesis in plant defense.

<https://doi.org/10.1371/journal.pgen.1010285.g006>

previous findings [51]. JA is known to promote dark-induced senescence [20], however, such a high content of JA in *SIJAZ11* overexpression transgenic lines is not consistent with previous research. JA sensitivity analysis (S9 Fig) indicated that *SIJAZ10* and *SIJAZ11* could actively repress the JA-responsive pathway. Additional JA treatment showed that *SIJAZ10* and *SIJAZ11* overexpressing transgenic lines could still keep anti-ageing at high JA levels through the regulation of the JA response.

It has long been known that high levels of JA are harmful to normal plant growth and development [52–54]. We note that such a model in which the JAV1-JAZ8-WRKY51 (JJW) complex binds and represses JA biosynthesis genes was proposed to repress the JA biosynthesis in *Arabidopsis* [37]. This yield is largely consistent with our experimentally observed results. During the course of studies, we found that *SIJAZ10* and *SIJAZ11* were expressed at lower levels and that *SIJAZ10* and *SIJAZ11* were susceptible to degradation under normal conditions. When plants respond to JA, JAZ proteins are recruited by COI1 to degradation [21, 49]. Taken together, our experiments showed that the SIJAV1-SIWRKY51 complex (JW complex) negatively regulated JA biosynthesis by direct binding of the W-box of the *SLAOC* promoter. These results of IBU-treated seedlings suggested that either knockout or overexpression of *SIJAZ10* or *SIJAZ11* increased JA sensitivity (S3 Fig). The inhibitory activity of the JW complex was lower than that of JJW of WT when *SIJAZ10* or *SIJAZ11* was knocked down and JAZ proteins repressed the transcription of JA-responsive genes when *SIJAZ10* or *SIJAZ11* was overexpressed. These data validate our hypothesis that *SIJAZ10* and *SIJAZ11* are not simply related to the JJW complex to regulate JA signalling pathway.

Given that JA content is normally present at low levels in normal plant growth, additional stimuli are required for the regulation of JA or JAZ protein mediated signalling. Although our research suggests some degree of functional redundancy between *SIJAZ10* and *SIJAZ11*, they are much different especially for regeneration. Wounding is a prerequisite for plant regeneration, and the dynamic JA wave responds to wounding by rapidly influencing auxin signalling [19]. Here, we show that the difference in JA levels may be the major contributor to regeneration between *SIJAZ10-OE* and *SIJAZ11-OE*. However, prolonged treatment with JA did not further promote antiaging or regeneration (S9 Fig). This revealed that plant regeneration did not appear to be simply a JA-mediated plant defence response. Additional efforts, the moving direction of electrical signals and the flow of Ca^{2+} waves verified this hypothesis (Fig 5). Furthermore, we found that the movement of electrical signals took priority over the flow of Ca^{2+} waves after wounding. On the basis of previous studies and our current results, we suggest that *SIJAZ11* responds preferentially to transport JA into the wound area by altering the electrical signals, and immediately following the Ca^{2+} wave, it also carries auxin to the wound margins in response to injury. Overall, the *SIJAZ11* mediated plant regeneration is a complex process that involves electrical signals, Ca^{2+} waves, hormone metabolism, hormone transport and transcriptional regulators.

When plants are pressed by an external stimulus, the autoimmune defence mechanism rapidly activates the JA signalling pathway to induce the regulation of JA-related functions, leading to defence responses against the stress. However, since JAZ proteins are vulnerable to degradation, how JAZ proteins maintain stability and function remains to be elucidated. Ribulose biphosphate carboxylase (Rubisco) is necessary for the survival of plants; thus, the robustness of the *rbcS* gene facilitates adaptation to drastic environmental changes or prevents loss of RBCS when some of the copies are lost. Although most studies of RBCS have focused on photosynthesis [55], some other published literature has shown that the expression of RBCS is affected by stress (ozone, drought, salt and metal) and wounding [56, 57]. Our studies indicate that *SIRbcs-3B* maintains the stability of the *SIJAZ11* protein for a certain period of time. *ERF109* (JA-responsive ethylene response factor 109) binds directly to the promoters of *ASA1*,

and is well known to promote lateral root formation and mediates crosstalk between JA signaling and auxin biosynthesis [15]. Our study also suggested that SIJAZ11 regulated regeneration by stimulating of *SIERF109* and *SIASA1* expression (S10 Fig).

After years of related studies, the mechanism of JA-elicited plant defence has been shown for clarity, and the JA signalling pathway is becoming more detailed. However, jasmonat-zim-domain protein (JAZ) is well-known to researchers as a transcriptional repressor of JA signaling, and the mechanisms underlying the regulation of plant defence remain unknown. In this study, we have uncovered a new model of the molecular mechanism for the stress-induced burst of JA responses based on the results of the previous study (Fig 6I): during the period of normal growth in plants, SIJAZ10 and SIJAZ11 can promote the inhibitory activity of SIJAV1-SIWRKY51 (JJW) to repress JA biosynthesis genes, which subsequently enables the plant to grow and develop normally with low JA levels; when plants are stimulated, SIJAZ11 rapidly triggers the electrical signals and Ca^{2+} waves to degrade SIJAV1, which in turn activates degradation of the JJW complex to activate JA biosynthesis genes. This eventually leads to the rapid burst of JA that activates the plant defence response; furthermore, we also found that SIRbcs-3B could bind to stabilize SIJAZ11 for a period of time, and this interaction could protect SIJAZ11 to play an adaptive role over a long period of time in JA-induced regeneration.

Supporting information

S1 Table. Primers used for construction of transgenic vector.

(DOCX)

S2 Table. Primers used for qRT-PCR analysis.

(DOCX)

S3 Table. Primers used for construction of subcellular localization assay.

(DOCX)

S4 Table. Primers used for construction of Y2H vectors.

(DOCX)

S5 Table. Primers used for construction of Pull-down assay.

(DOCX)

S6 Table. Primers used for construction of Y1H.

(DOCX)

S7 Table. Primers used for construction of Vitro Degradation Assays.

(DOCX)

S1 Fig. Comparison of survival of WT and transgenic lines.

(TIF)

S2 Fig. Comparison of transcriptome data analysis of WT and transgenic lines. (a) Volcano plot for differential gene expression. (b) GO enrichment analysis. (c) KEGG and KEGG enrichment analysis of the DEPs.

(TIF)

S3 Fig. Comparison of IBU and TIBA treatment of WT and transgenic lines.

(TIF)

S4 Fig. Co-immunoprecipitation (Co-IP) studies.

(TIF)

S5 Fig. Yeast one-hybrid analysis.

(TIF)

S6 Fig. Transcriptional activity assay of JJW.

(TIF)

S7 Fig. Dual luciferase reporter gene assay and quantitative PCR. (a) Binds the *SLAOC* and *SLAOS* promoter region. (b) SIJAZ10-SIJAV1-SIWRKY51 and SIJAZ11-SIJAV1-SIWRKY51-complex effectively suppresses the expression of *SLAOS_{Pro}-LUC* in *N. benthamiana* transient expression assay. (c) Relative gene expression of *SLAOC* and *SLAOS* in WT, *sljaz10*, *SIJAZ10*-OE, *sljaz11* and *SIJAZ11*-OE.

(TIF)

S8 Fig. Ca²⁺ alter transcriptional repression of SIJAZ10-SIJAV1-SIWRKY51 and SIJAZ11-SIJAV1-SIWRKY51 complex on the *SLAOS_{Pro}-LUC* expression.

(TIF)

S9 Fig. Comparison of JA treatment of WT and transgenic lines.

(TIF)

S10 Fig. Quantitative PCR of *SIERF109* and *SIASA1*.

(TIF)

Author Contributions

Conceptualization: Boyan Tang, Tingting Tan, Yating Chen, Zongli Hu, Qiaoli Xie, Xiaohui Yu, Guoping Chen.

Data curation: Zongli Hu, Qiaoli Xie, Xiaohui Yu, Guoping Chen.

Formal analysis: Boyan Tang, Xiaohui Yu, Guoping Chen.

Funding acquisition: Zongli Hu, Xiaohui Yu, Guoping Chen.

Investigation: Boyan Tang, Qiaoli Xie, Xiaohui Yu, Guoping Chen.

Methodology: Tingting Tan, Yating Chen.

Project administration: Xiaohui Yu, Guoping Chen.

Resources: Boyan Tang, Xiaohui Yu, Guoping Chen.

Software: Boyan Tang, Tingting Tan, Yating Chen.

Supervision: Zongli Hu, Xiaohui Yu, Guoping Chen.

Validation: Boyan Tang, Tingting Tan, Yating Chen.

Visualization: Boyan Tang, Tingting Tan, Yating Chen.

Writing – original draft: Boyan Tang, Guoping Chen.

Writing – review & editing: Boyan Tang, Xiaohui Yu, Guoping Chen.

References

1. Yang S, Seo P, Yoon H, Park C. The arabidopsis NAC transcription factor VNI2 integrates abscisic acid signals into leaf senescence via the COR/RD Genes. *Plant Signal Behav.* 2011; 23(6): 2155–2168. <https://doi.org/10.1105/tpc.111.084913> PMID: 21673078

2. Heyman J, Cools T, Canher B, Shavialenka S, Traas J, Vercauteren I, Van den Daele H, et al. The heterodimeric transcription factor complex ERF115–PAT1 grants regeneration competence. *Nat Plants*. 2016; 2: 165–172. <https://doi.org/10.1038/nplants.2016.165> PMID: 27797356
3. Gan S. Making sense of senescence. *Plant Physiology*. 1997; 113: 313–319. <https://doi.org/10.1104/pp.113.2.313> PMID: 12223609
4. Woo H, Kim H, Nam H, Lim P. Plant leaf senescence and death-regulation by multiple layers of control and implications for aging in general. *Journal of Cell Science*. 2013; 126: 4823–4833. <https://doi.org/10.1242/jcs.109116> PMID: 24144694
5. Lim P, Kim H, Gil N. Leaf Senescence. *Annu Rev Plant Biol*. 2007; 58(1): 115–136.
6. Yu J, Zhang Y, Di C, Zhang Q, Zhang K, Wang C, et al. JAZ7 negatively regulates dark-induced leaf senescence in Arabidopsis. *Journal of Experimental Botany*. 2015; 67(3): 751–762. <https://doi.org/10.1093/jxb/erv487> PMID: 26547795
7. Jing H, Schippers J, Hille J, Dijkwel P. Ethylene-induced leaf senescence depends on age-related changes and OLD genes in Arabidopsis. *Journal of Experimental Botany*. 2005; 56(421): 2915–2923. <https://doi.org/10.1093/jxb/eri287> PMID: 16172137
8. Hong Y, Zhang Y, Sittipun S, Yu N, Zhan X, Shen X, et al. Premature leaf senescence 3, encoding a methyltransferase, is required for melatonin biosynthesis in rice. *Plant J*. 2018; 95(5): 877–891. <https://doi.org/10.1111/tpj.13995> PMID: 29901843
9. Bai J, Zhu X, Wang Q, Zhang J, Chen H, Dong G, et al. Rice TUTOU1 encodes a suppressor of cAMP receptor-like protein that is important for actin organization and panicle development. *Plant Physiology*. 2015; 169(2): 1179–1191. <https://doi.org/10.1104/pp.15.00229> PMID: 26243616
10. Kong Z, Li M, Yang W, Xu W, Xue Y. A novel nuclear-localized CCCH-type zinc finger protein, OsDOS, is involved in delaying leaf senescence in rice. *Plant Physiology*. 2006; 141(4): 1376–1388. <https://doi.org/10.1104/pp.106.082941> PMID: 16778011
11. Ye B, Shang G, Pan Y, Xu Z, Zhou C, Mao Y, et al. AP2/ERF transcription factors integrate age and wound signals for root regeneration. *Plant Cell*. 2019; 32(1): 226–241. <https://doi.org/10.1105/tpc.19.00378> PMID: 31649122
12. Sugiyama M. Organogenesis in vitro. *Curr Opin Plant Biol*. 1999; 2(1): 61–64. [https://doi.org/10.1016/s1369-5266\(99\)80012-0](https://doi.org/10.1016/s1369-5266(99)80012-0) PMID: 10047565
13. Niyogi K, Fink G. Two anthranilate synthase genes in Arabidopsis: defense-related regulation of the tryptophan pathway. *Plant Cell* 1992; 4(6): 721–733. <https://doi.org/10.1105/tpc.4.6.721> PMID: 1392592
14. Sun J, Xu Y, Ye S, Jiang H, Chen Q, Zhou W, et al. Arabidopsis ASA1 is important for jasmonate-mediated regulation of auxin biosynthesis and transport during lateral root formation. *Plant Cell* 2009; 21(5): 1495–1511. <https://doi.org/10.1105/tpc.108.064303> PMID: 19435934
15. Cai X, Xu P, Zhao P, Liu R, Yu L, Xiang C. Arabidopsis ERF109 mediates cross-talk between jasmonic acid and auxin biosynthesis during lateral root formation. *Nat Commun*. 2014; 5(5): 5833–5846. <https://doi.org/10.1038/ncomms6833> PMID: 25524530
16. Zhang G, Zhao F, Chen L, Pan Y, Sun L, Bao N, et al. Jasmonate-mediated wound signalling promotes plant regeneration. *Nat Plants*. 2019; 5: 491–497. <https://doi.org/10.1038/s41477-019-0408-x> PMID: 31011153
17. Gilroy S, Bialasek M, Suzuki N, Górecka M, Devireddy A, Karpinski S, et al. ROS, calcium, and electric signals: key mediators of rapid systemic signaling in plants. *Plant Physiology*. 2016; 173(3): 1606–1615.
18. Kazan K. Diverse roles of jasmonates and ethylene in abiotic stress tolerance. *Trends Plant Sci*. 2015; 20(4): 219–229. <https://doi.org/10.1016/j.tplants.2015.02.001> PMID: 25731753
19. Koo A, Howe G. The wound hormone jasmonate. *Phytochemistry*. 2009; 69(13–14): 1571–1580. <https://doi.org/10.1016/j.phytochem.2009.07.018> PMID: 19695649
20. Zhuo M, Sakuraba Y, Yanagisawa S. A jasmonate-activated MYC2-Dof2.1-MYC2 transcriptional loop promotes leaf senescence in Arabidopsis. *Plant Cell*. 2019; 32(1): 242–262. <https://doi.org/10.1105/tpc.19.00297> PMID: 31641025
21. Chini A, Fonseca S, Fernandez G, Adie B, Chico JM, Lorenzo O, et al. The JAZ family of repressors is the missing link in jasmonate signalling. *Nature*. 2007; 448(7154): 666–671. <https://doi.org/10.1038/nature06006> PMID: 17637675
22. Hu Y, Jiang Y, Han X, Wang H, Pan J, Yu D. Jasmonate regulates leaf senescence and tolerance to cold stress: crosstalk with other phytohormones. *Journal of Experimental Botany*. 2017; 68(6): 1361–1369. <https://doi.org/10.1093/jxb/erx004> PMID: 28201612

23. Browse John. Jasmonate Passes Muster: A Receptor and Targets for the Defense Hormone. *Annu Rev Plant Biol.* 2009; 60(1): 183–205. <https://doi.org/10.1146/annurev.arplant.043008.092007> PMID: 19025383
24. Koo A, Gao X, Jones A, Howe G. A rapid wound signal activates the systemic synthesis of bioactive jasmonates in Arabidopsis. *Plant J.* 2010; 59(6): 974–986.
25. Birnbaum K, Alvarado A. Slicing across kingdoms: regeneration in plants and animals. *Cell.* 2008; 132(4): 697–710. <https://doi.org/10.1016/j.cell.2008.01.040> PMID: 18295584
26. Chen L, Sun B, Xu L, Liu W. Wound signaling: The missing link in plant regeneration. *Plant Signal Behav.* 2016; 11(10): 4273–4276. <https://doi.org/10.1080/15592324.2016.1238548> PMID: 27662421
27. Ikeuchi M, Iwase A, Rymen A, Lambolez A, Kojima M, Takebayashi Y, et al. Wounding triggers callus formation via dynamic hormonal and transcriptional changes. *Plant Physiology.* 2017; 175(3): 1158–1174. <https://doi.org/10.1104/pp.17.01035> PMID: 28904073
28. Wasternack C, Hause B. Jasmonates: biosynthesis, perception, signal transduction and action in plant stress response, growth and development. An update to the 2007 review in *Annals of Botany.* *Annals of botany.* 2018; 111(6): 1021–1058.
29. Dombrecht B, Xue G, Sprague S, Kirkegaard J, Ross J, Reid J, et al. MYC2 differentially modulates diverse jasmonate-dependent functions in Arabidopsis. *Plant Cell.* 2007; 19(7): 2225–2245. <https://doi.org/10.1105/tpc.106.048017> PMID: 17616737
30. Zhang F, Yao J, Ke J, Zhang L, Lam V, Xin X, et al. Structural basis of JAZ repression of MYC transcription factors in jasmonate signalling. *Nature.* 2015; 525: 269–273. <https://doi.org/10.1038/nature14661> PMID: 26258305
31. Goossens J, Mertens J, Goossens A. Role and functioning of bHLH transcription factors in jasmonate signalling. *Journal of Experimental Botany.* 2017; 68(6): 1333–1347. <https://doi.org/10.1093/jxb/erw440> PMID: 27927998
32. Wu F, Deng L, Zhai Q, Zhao J, Li C. Mediator subunit MED25 couples alternative splicing of JAZ genes with fine tuning jasmonate signaling. *Plant Cell.* 2019; 32(2): 429–448. <https://doi.org/10.1105/tpc.19.00583> PMID: 31852773
33. Fernandez-Calvo P, Chini A, Fernandez-Barbero G, Chico J, Gimenez-Ibanez S, Geerinck J, et al. The Arabidopsis bHLH transcription factors MYC3 and MYC4 are targets of JAZ repressors and act additively with MYC2 in the activation of jasmonate responses. *Plant Cell.* 2011; 23(2): 701–715. <https://doi.org/10.1105/tpc.110.080788> PMID: 21335373
34. Sun J, Jiang H, Li C. Systemin/jasmonate-mediated systemic defense signaling in tomato. *Mol Plant.* 2011; 4(4): 607–615. <https://doi.org/10.1093/mp/ssr008> PMID: 21357647
35. Coolen S, Proietti S, Hickman R, Olivas N, Huang P, Verk M, et al. Transcriptome dynamics of Arabidopsis during sequential biotic and abiotic stresses. *Plant J.* 2016; 86(3): 249–267. <https://doi.org/10.1111/tpj.13167> PMID: 26991768
36. Mao J, Miao Z, Wang Z, Yu L, Cai X, Xiang C, et al. Arabidopsis erf1 mediates cross-talk between ethylene and auxin biosynthesis during primary root elongation by regulating *asa1* expression. *Plos Genetics.* 2016; 12(1): 5760–5780.
37. Yan C, Fan M, Yang M, Zhao J, Zhang W, Su Y, et al. Injury activates ca^{2+} /calmodulin-dependent phosphorylation of JAV1-JAZ8-WRKY51 complex for jasmonate biosynthesis. *Mol Cell.* 2018; 70(1): 136–149. <https://doi.org/10.1016/j.molcel.2018.03.013> PMID: 29625034
38. Zhou W, Lozano-Torres J, Blilou I, Zhang X, Zhai Q, Geert S, et al. A jasmonate signaling network activates root stem cells and promotes regeneration. *Cell.* 2019; 177(4): 942–956. <https://doi.org/10.1016/j.cell.2019.03.006> PMID: 30955889
39. Yu G, Wang L, Han Y, He Q. clusterProfiler: an R package for comparing biological themes among gene clusters. *J. Integr. OMICS.* 2012; 16(5): 284–287.
40. Altermann E, Klaenhammer T. PathwayVoyager: pathway mapping using the Kyoto Encyclopedia of Genes and Genomes (KEGG) database. *Bmc Genomics.* 2005; 6(1): 60–67. <https://doi.org/10.1186/1471-2164-6-60> PMID: 15869710
41. Liu N, Cheng F, Zhong Y, Guo X. Comparative transcriptome and coexpression network analysis of carpel quantitative variation in *Paeonia rockii*. *Bmc Genomics.* 2019; 20(1): 683–701. <https://doi.org/10.1186/s12864-019-6036-z> PMID: 31464595
42. Iske J, Seyda M, Heinbokel T, Maenosono R, Minami k, Nian Y, et al. Senolytics prevent mt-DNA-induced inflammation and promote the survival of aged organs following transplantation. *Nat Commun.* 2020; 11(1): 4289–4302. <https://doi.org/10.1038/s41467-020-18039-x> PMID: 32855397
43. Park J, Halitschke R, Kim H, Baldwin I, Feyereisen R. A knock-out mutation in allene oxide synthase results in male sterility and defective wound signal transduction in Arabidopsis due to a block in

- jasmonic acid biosynthesis. *Plant J*. 2002; 31(1): 1–12. <https://doi.org/10.1046/j.1365-313x.2002.01328.x> PMID: 12100478
44. Dindas J, Scherzer S, Mrg R, Von M, Müller H, Kas A, et al. AUX1-mediated root hair auxin influx governs SCFTIR1/AFB-type Ca²⁺-signaling. *Nat Commun*. 2018; 9(1): 1174–1184. <https://doi.org/10.1038/s41467-018-03582-5> PMID: 29563504
 45. Mousavi S, Chauvin A, Pascaud F, Kellenberger S, Farmer E. Glutamate receptor-like genes mediate leaf-to-leaf wound signalling. *Nature*. 2013; 500(7643): 422–426. <https://doi.org/10.1038/nature12478> PMID: 23969459
 46. Sasanuma T. Characterization of the rbcS multigene family in wheat: subfamily classification, determination of chromosomal location and evolutionary analysis. *Mol Genet Genomics*. 2001; 265(1): 161–171. <https://doi.org/10.1007/s004380000404> PMID: 11370863
 47. Creelman R, Mullet J. Biosynthesis and action of jasmonates in plants. *Annu Rev Plant Physiol Plant Mol Biol*. 1997; 48: 355–381. <https://doi.org/10.1146/annurev.arplant.48.1.355> PMID: 15012267
 48. Breeze E, Harrison E, Mchattie S, Hughes L, Hickman R, Hill C, et al. High-resolution temporal profiling of transcripts during arabidopsis leaf senescence reveals a distinct chronology of processes and regulation. *Plant Cell*. 2011; 23(3): 873–894. <https://doi.org/10.1105/tpc.111.083345> PMID: 21447789
 49. Thines B, Katsir L, Melotto M, Niu Y, Mandaokar A, Liu G, et al. JAZ repressor proteins are targets of the SCF(COI1) complex during jasmonate signalling. *Nature*. 2007; 448(7154): 661–665. <https://doi.org/10.1038/nature05960> PMID: 17637677
 50. Chung H, Howe G. A critical role for the TIFY motif in repression of jasmonate signaling by a stabilized splice variant of the JASMONATE ZIM-domain protein JAZ10 in arabidopsis. *Plant Cell*. 2009; 21(1): 131–145. <https://doi.org/10.1105/tpc.108.064097> PMID: 19151223
 51. Jiang Y, Liang G, Yang S, Yu D. Arabidopsis WRKY57 functions as a node of convergence for jasmonic acid- and auxin-mediated signaling in jasmonic acid-induced leaf senescence. *Plant Cell*. 2014; 26(1): 230–245. <https://doi.org/10.1105/tpc.113.117838> PMID: 24424094
 52. Huot B, Yao J, Montgomery B, He S. Growth-defense tradeoffs in plants: a balancing act to optimize fitness. *Mol Plant*. 2014; 7(8): 1267–1287. <https://doi.org/10.1093/mp/ssu049> PMID: 24777989
 53. Campos M, Kang J, Howe G. Jasmonate-triggered plant immunity. *J Chem Ecol*. 2014; 40(7): 657–675. <https://doi.org/10.1007/s10886-014-0468-3> PMID: 24973116
 54. Gimenez-Ibanez S, Boter M, Solano R. Novel players fine-tune plant trade-offs. *Essays Biochem*. 2015; 58: 83–100. <https://doi.org/10.1042/bse0580083> PMID: 26374889
 55. Khrebtkova I, Spreitzer R. Elimination of the Chlamydomonas gene family that encodes the small subunit of ribulose-1,5-bisphosphate carboxylase/oxygenase. *Proc Natl Acad Sci U S A*. 1996; 93(24): 13689–13693. <https://doi.org/10.1073/pnas.93.24.13689> PMID: 8942995
 56. Gesch R., Boote K, Vu J, Allen L, Bowes G. Changes in growth CO₂ result in rapid adjustments of ribulose-1,5-bisphosphate carboxylase/oxygenase small subunit gene expression in expanding and mature leaves of rice. *Plant Physiology*. 1998; 118(2): 532–529.
 57. Shen S, Jing Y, Kuang T. Proteomics approach to identify wound-response related proteins from rice leaf sheath. *Proteomics*. 2003; 3(4): 527–535. <https://doi.org/10.1002/pmic.200390066> PMID: 12687619